Influence of Supercritical CO_2 on the Interactions Between Maleated Polypropylene and Alkyl-Ammonium Organoclay

J. Liu,[1] M. R. Thompson,[1] M. P. Balogh,[2] R. L. Speer Jr.,[2] P. D. Fasulo,[2] W. R. Rodgers[2]

[1]*MMRI/ CAPPA-D, Department of Chemical Engineering, McMaster University, Hamilton, Ontario, Canada L8S 4L7*
[2]*General Motors R&D Center, Warren, Michigan 48090-9055*

Received 25 November 2009; accepted 11 June 2010
DOI 10.1002/app.32947
Published online 27 August 2010 in Wiley Online Library (wileyonlinelibrary.com).

ABSTRACT: Supercritical carbon dioxide ($scCO_2$) has been proposed as an effective exfoliating agent for the preparation of polymer-layered silicate nanocomposites, though there is limited fundamental understanding of this mechanism. This study looks at the interactions of this unique green solvent with three maleated polypropylenes of varying anhydride content and molecular size with an alkyl-ammonium organoclay. Mixtures of compatibilizers and organoclay were melt-annealed in a high pressure batch vessel at 200°C and subjected to either a blanket of nitrogen or $scCO_2$ at a pressure of 9.7 MPa. The structures and properties of these melt-annealed mixtures were characterized by X-ray diffraction, transmission electron microscopy, Fourier Transform infrared spectroscopy, nuclear magnetic resonance spectroscopy, differential scanning calorimetry, and contact angle measurement. The results indicate that the plasticizing influence of $scCO_2$ aided intercalation and exfoliation for intercalants of moderate molecular size and anhydride content which would otherwise have limited diffusion into the clay galleries.
 J Appl Polym Sci 119: 2223–2234, 2011

Key words: supercritical carbon dioxide; maleated polypropylene; organoclay

INTRODUCTION

For the polymer components that make a polymer-layered silicate (PLS) nanocomposite, it is well recognized in the foams literature that supercritical carbon dioxide ($scCO_2$) has a plasticizing effect, provided sufficient CO_2-philicity is demonstrated.[1–3] For olefinic polymers like polyethylene and polypropylene, $scCO_2$ demonstrates modest solubility in the range of 1–10 wt %, depending on the system conditions.[4] The result of this plasticizing effect during compounding, or other polymer processing operations, is most generally associated with a reduction of viscosity on the order of 10–30%, which can be attributed to the increased free volume of the melt.[5] Conversely, the compatibilizing additive commonly used with current polyolefin nanocomposite formulations still remains poorly understood with regard to its function in the mechanism of clay delamination, and its interactions with $scCO_2$ have thus far not been reported in the literature.

The term *compatibilizer*, when used in commercial nanocomposite literature, refers to a functionalized polymer with its backbone structure similar to the matrix resin and containing chemical groups suited to interfacial association with organo-modified clays. Because of its reasonable affinity with the matrix and clay species, minimal influence on final material properties, and ready availability, a popular example of a compatibilizer is maleic anhydride-grafted polypropylene (MA-PP).[6–9] It is believed that the anhydride moiety coordinates with the broken plane of the silicate tactoids which contains hydroxyl groups and other oxidative functionalities.[9–11] The exact influence of MA-PP on forming a nanocomposite remains a contentious subject in the literature since both its molecular weight and degree of functionalization are thought to contribute to the delamination mechanism of melt intercalation[9,10,12]; but, these two factors are highly correlated due to the degradation reaction used in its preparation.[13] It has been found that higher grafted concentrations of maleic anhydride lead to greater intercalation capacity,[9] but miscibility of the compatibilizer with the polymer matrix decreases and eventually domain segregation occurs.[10] On the other hand, as the degree of functionalization increases there is a corresponding

Correspondence to: M. R. Thompson (mthomps@mcmaster.ca).

Contract grant sponsors: Natural Science and Engineering Research Council (NSERC) of Canada, General Motors of Canada Limited (GMCL), Ontario's Initiative for Automotive Manufacturing Innovation (IAMI).

TABLE I
Properties of the Three Compatibilizers

Compatibilizer	Name	Melting range (°C)	Zero shear viscosity[a] (Pa s)	M_N (g/mol)	M_W (g/mol)	MA content (wt %)
Licocene® PP MA 6252[b]	Li6252	105–138	0.7	2,420	5,490	4.7 ± 0.2
Polybond® 3200[c]	PB3200	134–168	200	27,360	87,670	1.1 ± 0.1
Polybond® 3002[c]	PB3002	135–172	3,600	51,830	254,350	0.4 ± 0.1

[a] Measured at 200°C.
[b] Supplied by Clariant.
[c] Supplied by Chemtura.

decrease in the molecular weight of the MA-PP which reportedly improves clay dispersion but subsequently deteriorates the mechanical properties of the nanocomposite.[12] With regard to $scCO_2$, we consider its possible effects on the compatibilizer to include plasticization, improved interfacial association of the anhydride with the clay, or direct chemical reaction/association between the CO_2 and anhydride. Most evidence regarding $scCO_2$ interactions with maleic anhydride (MA) can be found in studies looking at Diels–Alder reactions conducted under supercritical conditions. Glebov et al.[14] found that the rate of reaction between maleic anhydride and isoprene under supercritical conditions was substantially increased when the MA concentration was below its CO_2 solubility limit and only a single phase existed. At higher concentrations of MA, multiple phases existed in their reaction system and the rate of reaction was decreased correspondingly closer to those trials without CO_2. Unfortunately, the literature in this area never hypothesized how the increase in reaction rate occurred. Extraction of MA from prepared MA-PP under $scCO_2$ was found by Clark and Lee,[15] but they provided little analysis on the mechanism. In the work of Liu et al.,[16] the authors attempted to prepare MA-PP by a solid-state free radical reaction aided by $scCO_2$. They found a maximum in the grafted maleic anhydride content in relation to CO_2 pressure, which was attributed to the partitioning of MA between different phases within the mixture.

This article presents our studies looking at the influence of $scCO_2$ on the diffusion-controlled interactions between an organoclay and various maleated polypropylenes. This is the third paper in a series attempting to understand the benefits of $scCO_2$ as a processing aid for producing highly exfoliated polyolefin nanocomposite materials.

EXPERIMENTAL

Materials

Three commercial maleated polypropylenes (MA-PP) were selected for this work to examine the influence of the maleic anhydride (MA) content and molecular weight on the intercalation of organoclays. These resins were Polybond® 3002 and Polybond® 3200 from Chemtura Corp., and Licocene® PP MA 6252 provided by Clariant Corp. Table I summarizes the properties of the three compatibilizers as well as lists the abbreviated terms used in this article to refer to each material. The measured MA content for each compatibilizer found in Table I was determined by KOH titration.

The organoclay, Cloisite® 20A (C20A) supplied by Southern Clay Products was selected based on its demonstrated favorable interactions with $scCO_2$ in our previous studies.[17] The clay species is a montmorillonite modified with dimethyl-dihydrogenated tallow ammonium chloride. Hydrogenated tallow is a mixture comprised largely of dimethyl-dioctadecylammonium chloride with minor components of dimethyl-octadecylhexadecylammonium chloride and dimethyl-dihexadecylammonium chloride. The properties of the organoclay are listed in Table II. The calculated spreading coefficients for the clay with each compatibilizer are listed in Table III, which showed that spontaneous spreading should be expected at the selected operating temperature of 200°C used in our experiments. The interfacial properties of each clay-compatibilizer combination used in the spreading coefficient were determined from contact angle measurements, following the method disclosed in reference.[18] Surface tension values of the clay and compatibilizers were determined using the sessile drop contact angle method at 50°C with 1-bromonaphthalene (dispersive component $\delta^d = 42.517$ mJ/m^2, polar component $\delta^p = 0.283$ mJ/m^2) and glycerin ($\delta^d = 35.541$ mJ/m^2, $\delta^p = 25.359$ mJ/m^2). The values were corrected to 200°C assuming

TABLE II
Properties of the Organic Modified Montmorillonite

Surfactant structure	Surfactant content (wt %)	Surfactant melting range (°C)	*d*-spacing (Å)
$(CH_3)_2$ $(HT)_2N^+Cl^-$	38.5 ± 0.2	25-60	25.8

HT, hydrogenated tallow ($C_{18} \sim 65\%$; $C_{16} \sim 30\%$; $C_{14} \sim 5\%$).

TABLE III
Surface Energy of the Three Compatibilizers and C20A and Interfacial Tension Between them at 50°C

Species	Dispersive contribution[a], γ^d (mJ/m^2)	Polar contribution[a], γ^p (mJ/m^2)	Total surface energy, γ (mJ/m^2)	Interfacial tension with C20A, γ_{sl} (mJ/m^2)	Spreading coefficient	
					λ_{12}	λ_{21}
Licocene 6252	35.8	0.9	36.7	0.0	1.3	−1.5
Polybond 3200	35.8	0.2	36.0	17.4	1.8	−2.4
Polybond 3002	36.1	0.1	36.2	28.4	1.4	−2.4
Cloisite 20A	37.34	0.7	38.1	–	–	–

[a] Standard deviation 0.8% (maximum).

a decrease in surface tension with temperature at a rate of 0.1 mJ/(m^2°C).[19]

The carbon dioxide and nitrogen used in the experiments were supplied by Air Liquide Canada at 99.5% and 99.995% purity, respectively.

Procedures

In preparation for the experiments, all three compatibilizers were first converted into fine powder from their pellet form to minimize segregation while being mixed with the clays. Li6252 was cryogenically ground into a fine powder of approximately 50 μm. The powders of PB3200 and PB3002 were prepared by precipitation from hot xylene using acetone due to difficulties with grinding, even under cryogenic conditions. The prepared materials were thoroughly washed with acetone, vacuum dried overnight at 80°C, and reduced to a fine powder in a blender to reach a particle size of 10–100 μm, similar to the clay. FTIR analysis confirmed that after powder formation the major absorbances for the grafted anhydride remained, namely carboxylic acid vibrations at 1715 cm^{-1} and the anhydride ring at 1781 cm^{-1} and 1790 cm^{-1}; the absorption pattern changed little when compared to the as-supplied compatibilizers. The MA-PP powder and clay powder were mixed manually to a ratio of 2 : 1 by weight. In certain instances, an organoclay that had been pretreated by exposure to $scCO_2$ (s-C20A) was used in place of C20A for the experiments. The pretreatment of the clay was performed by soaking the C20A under 9.7 MPa of $scCO_2$ at 200°C in a batch vessel for 3 h followed by a rapid depressurization at ~ 10 MPa/s.

Trials were run varying the compatibilizer, clay type, or gas type present. As typical conditions, each prepared polymer mixture of MA-PP and organoclay was first dried at 40°C under vacuum overnight and then directly placed into a high pressure batch vessel that had been heated to 200°C. The duration of an experiment was 30 min once pressurization was achieved. The apparatus has been described in detail in an earlier paper.[17] For those runs involving $scCO_2$, the gas was injected and maintained at 9.7 MPa over the course of the trial with a Teledyne-ISCO 260D syringe pump. At the end of the run, the gas was removed by depressurization at 4.8 MPa/s. For each trial condition performed with $scCO_2$, a corresponding trial run under a nitrogen blanket was prepared for comparison and to establish the temperature effects while minimizing oxidative degradation. Upon removal from the batch vessel, each sample was ground using a mortar and pestle for subsequent analyzes.

Characterization

Thermal properties of the clay and polymers were measured in a TA Instruments Q200 differential scanning calorimeter (DSC). Thermograms of the different MA-PP by DSC were collected under a nitrogen atmosphere during the second heating cycle at a ramp rate of 10°C/min. The melting ranges for the three compatibilizers are given in Table I. The thermal shielding of the intercalated surfactant in the clay required a more sensitive approach; therefore, the modulating option of the DSC was used with a modulated period and amplitude of 60 s and 1°C, respectively, at a heating rate of 1°C/min. The determined melting transition for the surfactant of the organoclay is included in Table II.

The molecular weight moments of each compatibilizer listed in Table I were determined using a high temperature gel permeation chromatograph (GPC) manufactured by PolymerChar and equipped with IR, viscosity, and light scattering detectors (15 and 90°). The analysis was conducted at the Institute of Polymer Research (University of Waterloo, Waterloo, ON). The columns were PLgelOlexis made by Polymer Laboratories, and the chromatograph was operated at 145°C. A sample was dissolved in trichlorobenzene and passed through the columns at a flow rate of 1 mL/min.

Direct observations of gallery spacing for the clay were made by powder X-ray diffraction (XRD) using Cu Kα radiation (λ = 1.541 Å). Both *ex-situ* and *in situ* analyses was conducted by XRD. The apparatus used for the *in situ* XRD study was described in detail in an earlier paper.[20] Briefly, the cell containing the clay samples for the *in situ* tests was a 1-mm

diameter quartz capillary tube (10 μm wall thickness) with its open end affixed to a high pressure manifold. The CO_2 gas was pressurized to above 13.9 MPa in an attached batch vessel and then supplied at the appropriate pressure by a series of control valves to the sample cell. The clay sample was heated by a small furnace encompassing the capillary tube. Two 90° conical windows cut into the furnace wall allowed observation of the 2θ ranges ±45° at 0° incidence angle. The temperature of the system was controlled by a thermocouple mounted in the wall of the furnace while the actual temperature of the sample in the field of view of the X-ray beam was calibrated using a series of melting point standards. The XRD data was collected over a period of 300 s with consecutive scans taken to study the influence of the gas on the clay/compatibilizer system for a 30-min duration.

Transmission electron microscope (TEM) analyses of the processed mixtures were performed using a JEOL 1200 EX TEMSCAN microscope operating at an accelerating voltage of 80 kV and a magnification of 200,000×. For TEM observations, each sample was first embedded in epoxy resin and microtomed with a diamond knife into thin sections approximately 70 nm thick.

Interactions between the organoclay with the different compatibilizers affected by the $scCO_2$ were determined by Fourier transform infrared (FTIR) and solid-state ^{13}C nuclear magnetic resonance (^{13}C-NMR) spectroscopy.

Transmission infrared absorbance spectra of the neat compatibilizers and prepared samples from the high-pressure vessel involved collection of 64 scans at 2 cm^{-1} resolution over a range of 500–4000 cm^{-1} using a Bio-Rad FTS-40 spectrometer. The neat compatibilizers were prepared as films in a hot press at 165°C under 0.13 MN compressive force for 5 min. Powder clay or powdered clay/polymer samples were mixed with dry KBr and compressed into tablets.

The 125 MHz solid-state ^{13}C-NMR analysis was performed with a Bruker 500 MHz NMR spectrometer at 23 and 50°C. The higher probe temperature used was higher than the melting point of the surfactant (45°C) for C20A. Both single-pulse direct-polarization (Bloch-decay) and cross-polarization methods were used with ^{1}H decoupling. All experiments employed a 24-kHz spectral window centered on the main peaks, a 5-kHz magic-angle spinning frequency, and a 41-ms acquisition time. A cross-polarization (CP MAS) contact time of 3 ms and repetition delay of 5 s were used for the spectra as determined by a variable contact-time experiment. A 4.5-μs (90°) ^{13}C pulse and a repetition delay of 40-s were used in the Bloch-decay (BD MAS) analysis. All chemical shifts were referenced to tetramethylsilane (TMS) at 0 ppm.

RESULTS AND DISCUSSION

Previous works by the present authors have examined the influence of $scCO_2$ on the organoclay individually, both after treatment in the supercritical solvent[17] and *in situ*.[20] Both experiments found the supercritical solvent primarily acted as a plasticizer with alkyl ammonium-modified montmorillonite, overcoming the "barrier effect." The barrier effect normally limits the cation exchange reaction used in their preparation to the outer edges of the clay galleries. The barrier is created by the presence of van der Waals attractive forces between bound and free intercalated surfactant species, thereby preventing the organic modifier from fully penetrating into the central region of the silicate sheets, and hence sodium ions remain present in the prepared organoclays. Supercritical CO_2 along with elevated temperatures allowed greater chain mobility for the surfactant molecules and as a result, further cation exchange reactions were observed to occur.[17] In general, this unique solvent afforded rearrangement of the surfactant and greater organic coverage over the silicate surface, which brought about either basal expansion or partial collapse depending on the original surfactant arrangement in the galleries. With rapid depressurization of the clay suspension in $scCO_2$, a small but further increase in basal spacing was detected, though the work of Horsch et al.[21] suggested instead that the particles were fractured. In the studies of this article, these rapidly depressurized $scCO_2$-treated organoclays are simply referred to as *pretreated* and the species included in the study is denoted as s-C20A. With the introduction of a compatibilizer to the system of organoclay and $scCO_2$, it is expected that both polymer intercalation and surfactant rearrangement will proceed simultaneously.

XRD, interlayer spacing of the mixtures

Direct evidence of intercalation by the compatibilizers was obtained from analysis of the XRD patterns for the melt-annealed mixtures and neat C20A under $scCO_2$ or N_2 conditions. First, the basal spacings of the neat organoclays as determined by *ex-situ* XRD analyses are shown in Figure 1. The as-supplied C20A showed a characteristic broad, moderate intensity peak centered at $2\theta = 3.4°$ corresponding to a nominal basal spacing of 26 Å. It is noted that the same clay material showed only minor basal expansion while heated to 200°C (while observed *in situ*, data not shown) due to melting of the surfactant with the characteristic peak shifted to $2\theta = 3.0°$ as well as showing greater layer-to-layer uniformity. Layer-to-layer uniformity in this case refers to a reduction in the full-width half-maximum (FWHM)

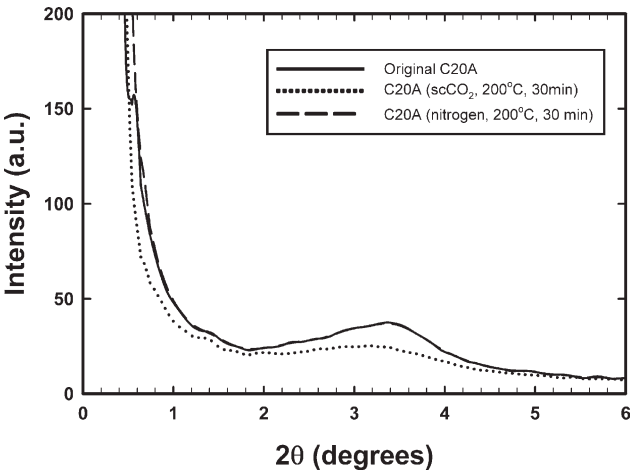

Figure 1 XRD patterns of C20A as-supplied in its original state, processed for 30 min in a $scCO_2$ atmosphere (200°C and 9.7 MPa), or processed for 30 min in a N_2 environment (200°C).

measure of peak breadth which diminished from 1.9° at room temperature to 1.2° once the system reached 200°C. Yet as noted in Figure 1 once removed from heat and measured *ex-situ* the diffraction pattern for the clay conditioned at 200°C under nitrogen for 30 min matched that of the as-supplied sample. Conversely, the *ex-situ* diffraction pattern of C20A after its suspension in $scCO_2$ at 200°C for 30 min and then removed, showed persistent expansion with a nominal peak position of $2\theta = 2.8°$ and a broader peak breadth (FWHM = 1.2°). With the increased packing density of surfactant gained by the organoclay while under the plasticizing influence of the supercritical solvent, the $scCO_2$ treated C20A retained its heat-expanded morphology upon cooling. The reduced intensity of the peak is attributed to the disturbed tactoid arrangement in the particles as the gas was released.[17] In comparison to these neat organoclay materials, the intercalated clay structures with the different compatibilizers showed much greater variance in the detected basal reflections.

Mixed with the low viscosity, highly maleated Li6252, the periodic structure of C20A was no longer detected by *ex-situ* XRD analyses for either $scCO_2$ or N_2 environments as seen in Figure 2. This oligomeric compatibilizer was found to be highly effective for clay intercalation but raised concerns for end-use suitability because of its low molecular weight. For the mixture of PB3002 and C20A, the diffraction peak shifted from a 2θ angle of 3.4° for the as-supplied organoclay to a lower 2θ angle of 3.0° with the aid of $scCO_2$, indicating that the nominal basal spacing of the clay increased to 29 Å. This increase in spacing was similar to the $scCO_2$-treated clay discussed in Figure 1, leaving doubts that intercalation occurred. Under the N_2 atmosphere, the basal spacing of the clay mixed with PB3002 was only 27 Å showing little difference from the as-supplied C20A. These outcomes indicated that the supercritical fluid continued to change the surfactant morphology of the organoclay within the mixture but the resulting expansion was insufficient to accommodate the large molecular size of the PB3002 intercalant. The TEM micrographs in Figure 3 for the $scCO_2$-treated mixtures with Li6252 and PB3002 support the observations by XRD. In the micrographs, the clay demonstrated an expanded sheet stack arrangement in the case of Li6252 while for the PB3002 mixture the ordered layer structure of the clay remained dense.

For the compatibilizer in the mid-range with respect to MA content and molecular weight, PB3200, the effect of $scCO_2$ on the mixture of C20A and compatibilizer was easily observed and significant. As shown in Figure 2, after annealing under nitrogen, the clay from this melt-annealed mixture showed a shift in its *ex-situ* diffraction peak to a 2θ

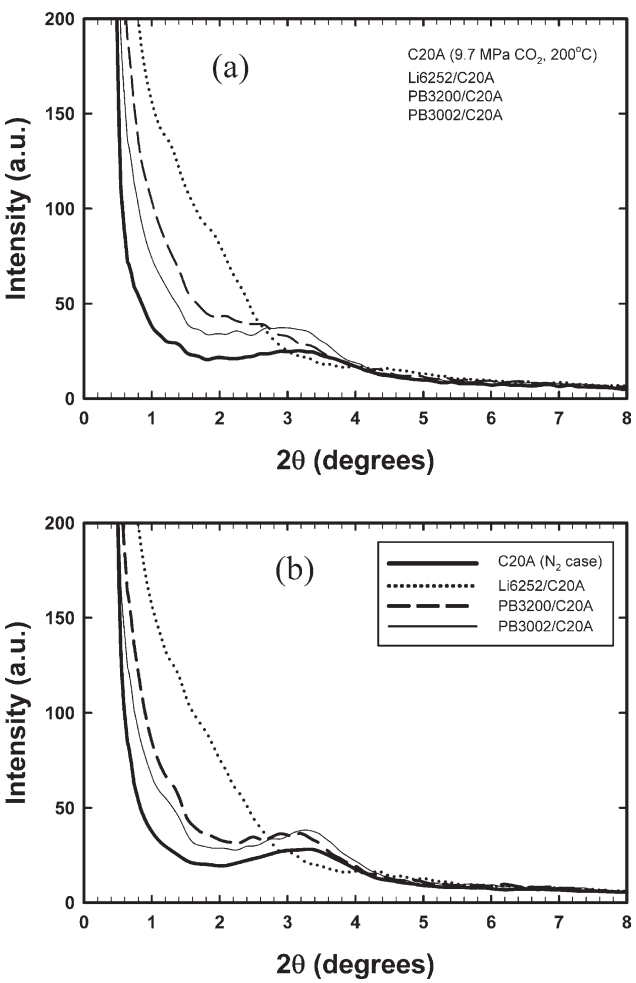

Figure 2 XRD patterns of C20A mixtures with Licocene 6252, Polybond 3200, and Polybond 3002 processed at 200°C for 30min for either (a) $scCO_2$ or (b) N_2, compared to their respective C20A processed under the same conditions.

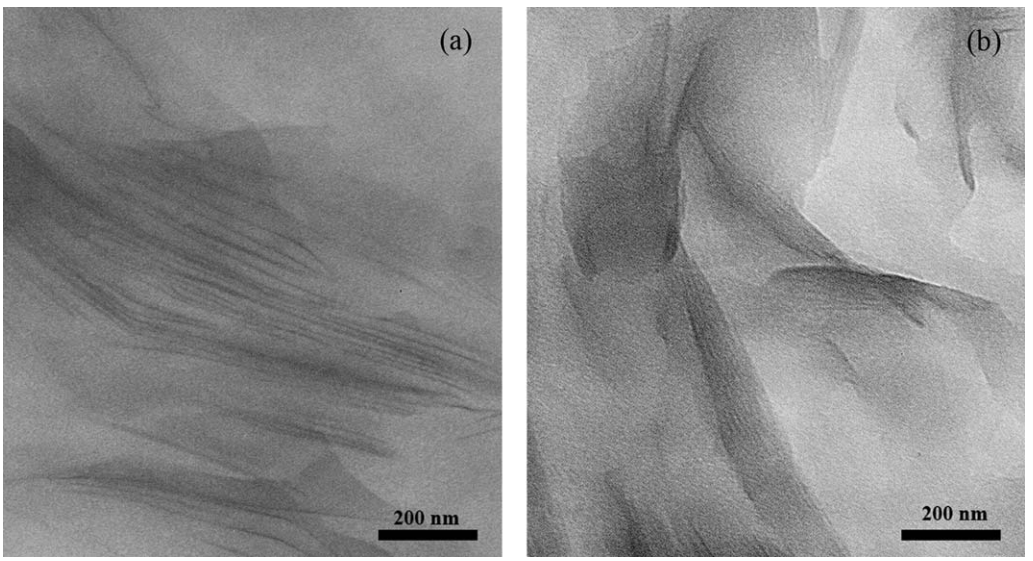

Figure 3 TEM micrographs for (a) Li6252/C20A mixture and (b) PB3002/C20A mixture, both processed under $scCO_2$.

angle of 3.0° (basal spacing of 29 Å) indicating that even without $scCO_2$ partial intercalation by this polymer species was possible. After annealing under $scCO_2$, the (001) peak for C20A appeared only as a shoulder at $2\theta = 2.5°$ but had become so wide that the 2θ position of the highest scattering intensity was almost indistinguishable from the background. The majority of the clay had lost its periodic stacked arrangement, which we attributed to substantial intercalation by the compatibilizer into the galleries of the clay. The structure of the system was analyzed further by FTIR and NMR and will be discussed in a later section. TEM micrographs of the $scCO_2$ treated PB3200 mixtures with C20A and s-C20A (which is discussed later in this section) are shown in Figure 4. The clay galleries seen in the micrograph for the mixture with C20A show good dispersion, though tactoids rather than platelets are observed.

To complement the *ex-situ* analysis mentioned earlier, the PB3200 mixture with C20A was evaluated using a specially constructed apparatus to observe the structure of the clay by XRD over time while under heat and pressure. Because of the fragile nature of the quartz tube used in the apparatus, the system could only reach a pressure of 8.4 MPa CO_2 at 200°C; however, such a condition still corresponds to the supercritical state of CO_2 and was felt to be sufficiently close to conditions used in the batch vessel to be meaningful. Figure 5 plots the nominal 001 peak position and its breadth (FWHM) for the clay within the mixture over time, either under atmospheric pressure or supercritical conditions. In the

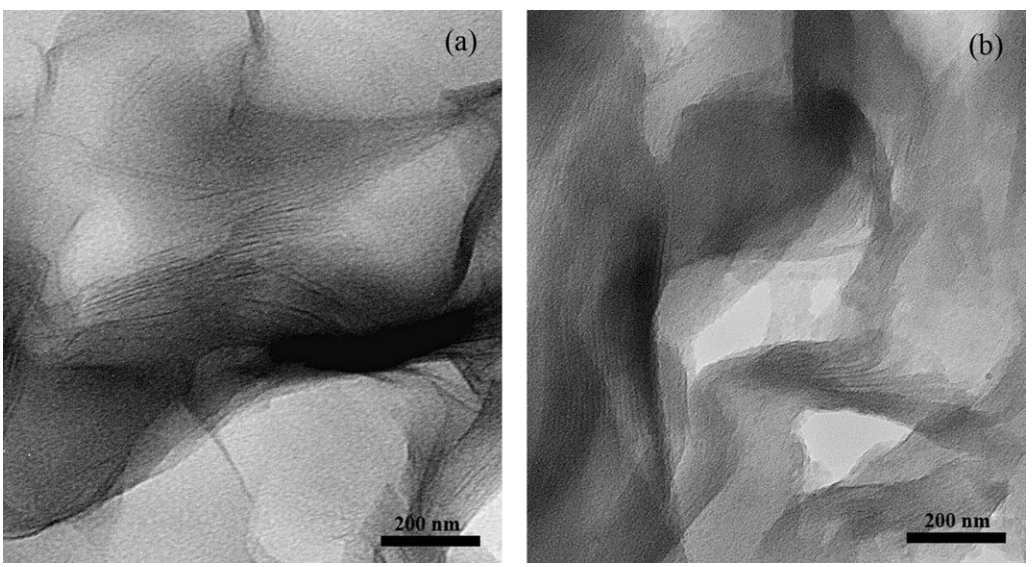

Figure 4 TEM micrographs for (a) PB3200/C20A, and (b) PB3200/s-C20A, both processed under $scCO_2$.

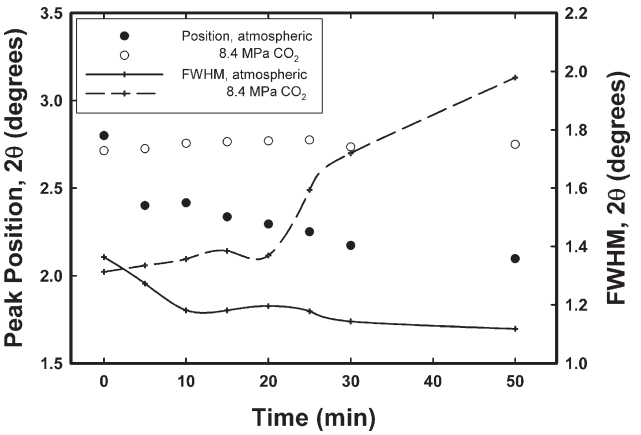

Figure 5 Changes in the nominal peak position and peak breadth (as measured by FWHM) while heated at 200°C for 30 min and then cooled to 50°C between 30 and 50 min for the PB3200/C20A mixture, with and without $scCO_2$.

absence of high pressure, steady diffusion of the compatibilizer into the clay is assumed as the (001) peak shifted from $2\theta = 2.8°$ to 2.2° over 30 min. During this period, an improvement in layer-to-layer uniformity was seen over the first 10 min of the test as the peak became narrower and then no further changes in its breadth occurred though the peak continued to shift to lower 2θ angles. Between 30 and 50 min, the sample was cooled to 50°C over which time no further changes in structure were observed. Comparatively, under $scCO_2$ the (001) peak for C20A remained nearly constant in position over the 30 min while at 200°C. At the same time, the peak breadth broadened significantly, particularly after an induction period of 20 min. The peak appeared to continuously broaden through the cooling stage between 30 and 50 min. The final peak position was 0.2° higher by these *in situ* experiments compared to the *ex-situ* analysis in Figure 2 but the peak broadening corresponds well. Although not included in this article, the same *in situ* trends for peak position and breadth, with and without $scCO_2$ were observed by the authors with a clay-compatibilizer mixture having a 50/50 w/w% composition.

Some of the discussion in the literature suggests that using a pretreated organoclay in place of the as-supplied species can further clay exfoliation in the final prepared nanocomposite without needing $scCO_2$ to be injected into the compounding process. This pretreated material should, in theory, remove the necessity for compounders to design and operate a supercritical gas delivery system. Figure 6 compares the *ex-situ* XRD diffraction patterns for the melt-annealed mixture of PB3200 with either the $scCO_2$ pretreated C20A (s-C20A) or the as-supplied C20A, processed under either N_2 or $scCO_2$ conditions. The two mixture compositions retrieved from the supercritical solvent displayed similar diffraction patterns with their (001) peaks seen only as shoulders from the baseline at $2\theta = 2.5°$. According to the TEM micrographs in Figure 4, the extent of exfoliation for the s-C20A mixture under $scCO_2$ was also similar to the C20A counterpart, with mostly clay tactoids visible and the largest interlayer expansion noted being approximately 92 Å. In general, qualitative observations afforded by TEM showed little difference between the two clay systems. The same two materials annealed under nitrogen showed more clearly defined peaks centered at $2\theta = 3.0°$ by XRD. However, the peak in Figure 6 appears broader for the mixture with the pretreated clay suggesting more ready disruption of the silicate stacking even under nitrogen. This was attributed to the more disordered tactoid arrangement of s-C20A creating more paths for intercalating polymer chains to enter the clay galleries.

Infrared spectroscopy

The FTIR spectra of the individual constituents are shown in Figure 7. The pretreated s-C20A was not included as its spectra matched that of C20A. The vibrations in the frequency ranges of 1400–1520 cm^{-1} and 2800–3000 cm^{-1} pertaining to CH_2 bending and stretching modes respectively, have been of interest to researchers attempting to identify structural changes in the clay pertaining to the surfactant and intercalating molecules.[22–24] From Figure 7, it can be seen that C20A had methylene modes centered at 1468, 2852, and 2921 cm^{-1} whereas for the MA-PP species, the detectable modes corresponded to 1460 (very broad), 2838, and 2917 cm^{-1}. The peaks at 2838 cm^{-1} for MA-PP and 2852 cm^{-1} for C20A were relatively sharp and remained well differentiated in the spectra for the mixtures, so these

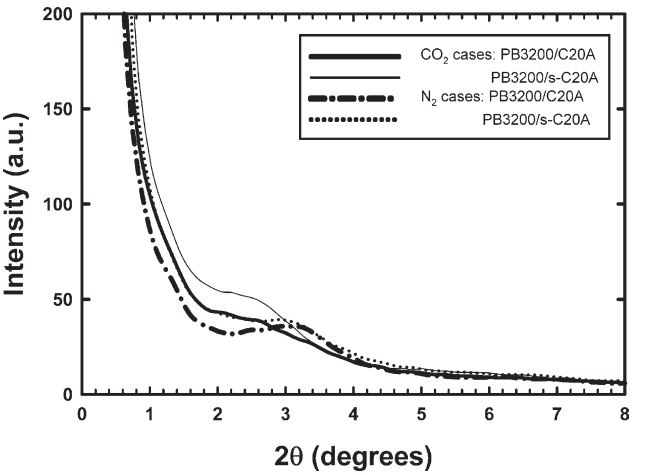

Figure 6 XRD patterns of PB3200 prepared mixtures with C20A and s-C20A under $scCO_2$ and N_2 conditions.

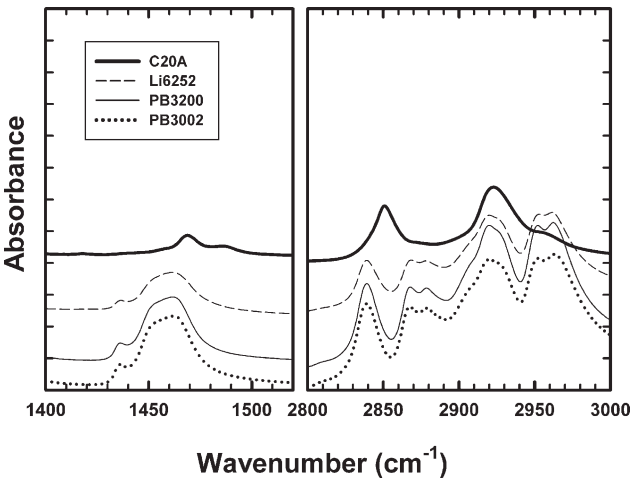

Figure 7 FTIR spectra at bands 1400-1520 cm^{-1} and 2800-3000 cm^{-1} for C20A and the three individual compatibilizers.

vibrations related to symmetric CH_2 stretching were selected to monitor changes in the systems as a result of $scCO_2$ treatment. The FTIR spectra of the three melt-annealed mixtures from the different compatibilizers, under N_2 or $scCO_2$ are shown in Figure 8. For the Li6252 derived mixtures, where the compatibilizer was observed by XRD to have fully intercalated into the galleries of C20A regardless of the supercritical fluid being present, the band at 2852 cm^{-1} could no longer be detected in the spectra. On the other hand, the band showed the least change for the mixture with PB3002 whose high-molecular weight chains were noted by XRD as being restricted from entering the galleries of the organoclay. However, the band still showed a markedly reduction with PB3002 when the mixture was processed with $scCO_2$ compared to N_2. The band intensity for the nitrogen case with PB3200 bore close similarity to the $scCO_2$ case for the PB3002-based mixture, in the same way as the XRD diffraction patterns between these two materials reported similar clay structures. In the presence of the supercritical solvent, the mixture prepared with PB3200 under $scCO_2$ showed the band at 2852 cm^{-1} to still be present though its intensity was almost negligible, similar to the Li6252-based material.

The band at 2852 cm^{-1} showed a marked correspondence with the extent of intercalation revealed in the diffraction patterns from the XRD results. The band decreased in its intensity as more chains intercalated into the galleries of C20A, disrupting the solid-like environment of the near *all-trans* alkyl surfactant.[22–24] The NMR analysis in the following section shall examine this change in microstructure more closely, enough to postulate a cause for the loss of this vibrational band in the spectra. The FTIR spectra for the melt-annealed mixtures in the frequency ranges of 400–1300 cm^{-1} and 1600–1900 cm^{-1} revealed no significant information which could discern the changes brought about by the gases within the resolution of the measurement (i.e., 2 cm^{-1}). The absorbance bands for the carboxylic acid groups (1715 cm^{-1}) and anhydride groups (1780–1792 cm^{-1}) of the compatibilizer did not significantly change in position or intensity after exposure to the two gases at 200°C. Therefore, no analysis regarding the hydrogen bonding of the anhydride moiety with the oxygen plane of the clay or the exfoliated silicate structure could be made by this technique. This could, in part, be attributed to the fact that the mixtures were poorly dispersed in the absence of shear.

NMR analysis

The conformation of the intercalated molecules (i.e., surfactant and compatibilizer) related to the use of the supercritical solvent in the preparation of nanocomposite materials was studied by variable-temperature solid-state ^{13}C-NMR experiments. Both common techniques, cross polarization (CP) MAS and Bloch decay (BD) MAS were used to probe the structural differences in the melt-annealed PB3200 mixtures and neat organoclay species prepared from the batch vessel. This allowed the products from the $scCO_2$ and N_2 environments to be compared. For clarity, this was an *ex-situ* analysis. The initial variable contact-time CP MAS experiments with the mixtures showed little difference between the samples processed with and without $scCO_2$. With varied contact times, both samples showed a rapid increase in signal intensity up to 1.2 ms contact time, and then a gradual decrease in intensity out to 5 ms which was set as the maximum contact time. The

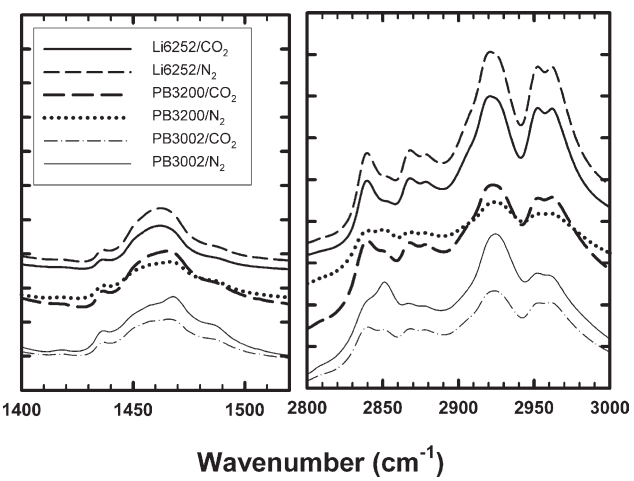

Figure 8 FTIR spectra at bands 1400-1520 cm^{-1} and 2800-3000 cm^{-1} for Li6252, PB3200, and PB3002 mixtures with C20A processed with and without $scCO_2$.

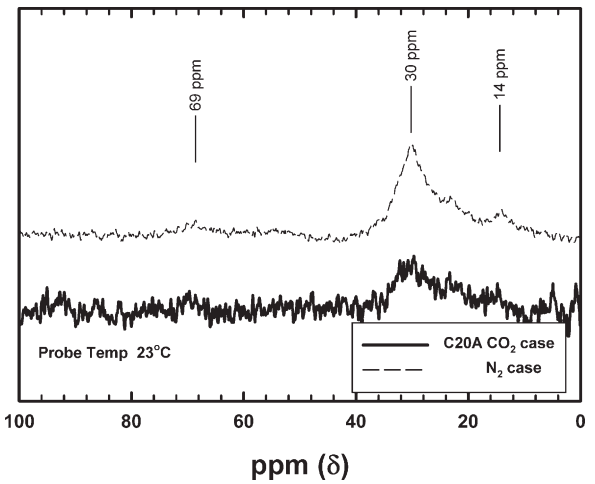

Figure 9 ^{13}C-NMR spectra of collected C20A processed under $scCO_2$ and N_2 using a probe temperature of 23°C.

lack of differentiation in the spectra for the two samples was attributed largely to inefficient cross-polarization of the surfactant intercalated within the clay in comparison to the detected chemical shifts assigned to isotactic polypropylene (22 ppm CH_3, 26 ppm CH, and 44 ppm CH_2) at both temperatures.

Comparatively, the Bloch-decay (BD MAS) technique showed discernable differences between the $scCO_2$ and N_2 processing conditions, most notably for the PB3200 mixture. The lengthy recycle delay for the direct-pulse technique (Bloch-decay) provided considerably more signal related to the confined surfactant compared to cross-polarization. The ^{13}C spectra prepared using the Bloch-decay method are shown in Figures 9 and 10 for the organoclay species and for the melt-annealed PB3200 mixtures, respectively. The spectra of the two neat organoclays after annealing in one of the two gas environments are shown in Figure 9. Both spectra showed similar detectable chemical shifts, though the poor signal-to-noise ratio for the neat paramagnetic material made quantitative assertions difficult. The majority of the surfactant was considered to be in the paraffin-type arrangement exhibiting solid-like mobility attributed to an *all-trans* chain conformation, agreeing with the corresponding XRD-detected gallery heights for the $scCO_2$-treated and nitrogen-treated C20A of 28 Å and 25 Å, respectively,.[17] The signals for the interior methylene groups in the alkyl chains of the surfactant were the most sensitive to the conformer state and in this regards, the peak at 30 ppm was assigned to the mixed conformation of trans and gauche of the internal methylenes and shoulder peak at ~ 33 ppm to the *all-trans* state of these groups.[23,25] The chemical shift observed at 14 ppm corresponded to the terminal methyl groups (C—CH_3) for both C_{18} and C_{16} alkyl chains. Both C_{18} and C_{16} chain lengths were present as the quaternary ammonium surfactant used for C20A was mainly composed of dimethyl-dioctadecyl-ammonium salt but included minor components of dimethyl-octadecyl-hexadecyl-ammonium and dimethyl-dihexadecyl-ammonium salts, and very low concentrations of dimethyl-octadecyl-ammonium and dimethyl-hexadecyl-ammonium salts. Several other peaks were identified but were much more difficult to distinguish from the baseline noise of the spectra, most likely due to the close proximity of these carbon groups to the paramagnetic influence of the montmorillonite sheets. Not seen in the plot were the terminal group signals due to their low intensity, though the resonance at 69 ppm corresponding to the methylenes attached to the nitrogen was just barely detected in this case. The weaker signal for the $scCO_2$ treated organoclay compared to nitrogen was attributed to both paramagnetic interference

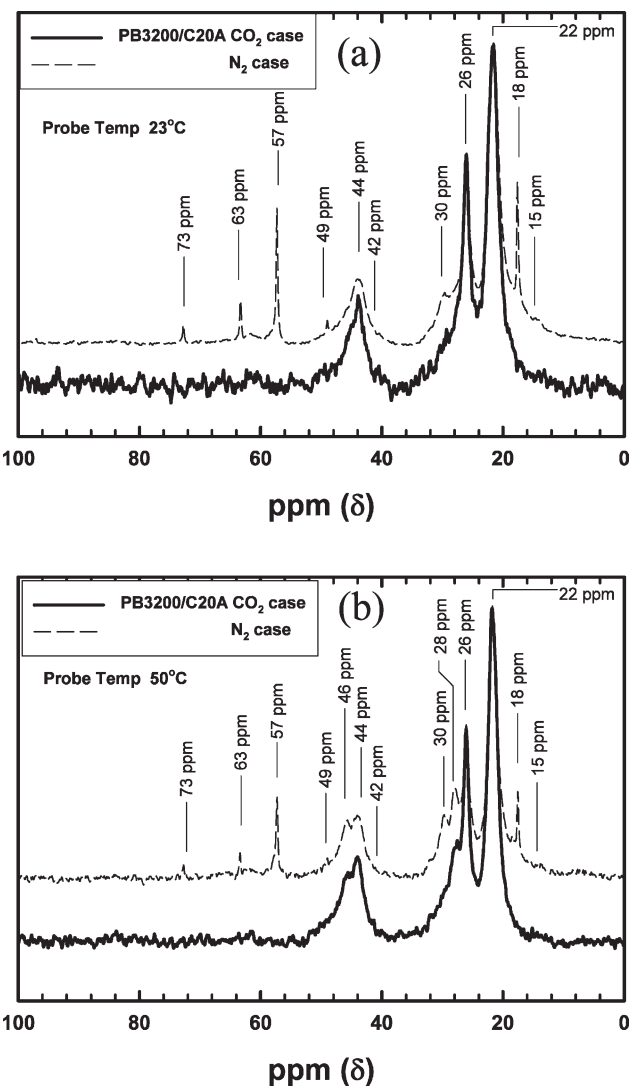

Figure 10 ^{13}C-NMR spectra for the PB3200/C20A mixture processed under $scCO_2$ and N_2,using a probe temperature of a) 23°C and b) 50°C.

from the silicate and the lower mobility of surfactant chains due to their greater packing density within the interlayer region.[17]

Figure 10(a,b) show the spectra for the PB3200 melt-annealed mixture using the BD MAS technique at NMR probe temperatures of 23 and 50°C, respectively. The spectra do not include the anhydride carbonyl resonances at 172–174 ppm which could not be distinguished from the baseline noise by this technique. The three isotactic polypropylene resonances were the most intense signals, but the resonance peaks attributed to the surfactant were clearly observable in the poorly intercalated mixture (i.e., sample processed with N_2). For this nitrogen-processed PB3200/C20A mixture, the signal for the interior methylene groups was observable as an overlapped shoulder peak with highest intensity at 30 ppm, similar to the neat clay shown in Figure 9, indicating that most of the surfactant remained in its original conformation in the presence of the compatibilizer. At the elevated probe temperature, 50°C, new methyne and methylene signals were detected at 28 ppm and 46 ppm, respectively, indicating an increased liquid-like state for the surfactant/compatibilizer mixture. A weak peak corresponding to the terminal propyl end group of the compatibilizer was observed at 15 ppm, whereas a strong terminal methyl signal for the surfactant was found downfield at 18 ppm. The peak at 57 ppm indicated that the nitrogen-bound methyl groups ($-N-CH_3$) were unaffected by the presence of the compatibilizer yet the peak representing the $N-CH_2-$ was shifted downfield to 73 ppm. The peaks at 49 and 63 ppm were assigned to the CH_2 and CH groups of the grafted anhydride ring.[26] In general, the spectra for the nitrogen-processed PB3200/C20A mixture indicated little disruption of the methylene conformation for the surfactant by the compatibilizer, confirming the XRD results of minimal intercalation by the MA-PP. The downfield shift of the carbon groups around the nitrogen group suggests the partial influence of hydrogen bonding by the anhydride moiety.

The spectrum for the more highly exfoliated PB3200/C20A mixture prepared under $scCO_2$ was included in Figure 10. At a probe temperature of 23°C, the chemical shifts at 22, 26, and 44 ppm were the strongest, corresponding to the compatibilizer, with an additional shoulder peak at 46 ppm and a barely detectable shoulder peak at 28 ppm. At the elevated probe temperature of 50°C the shoulder peaks at 28 ppm was more clearly defined. The resonances corresponding to the alkyl surfactant were not detected in the ^{13}C spectra for either probe temperature. The disappearance of these alkyl-related resonances can be explained by the surfactant being forced into a disorganized lateral bilayer arrangement to accommodate the inclusion of the intercalated compatibilizer species. In the molecular simulations of Toth et al.,[27] it was observed that in the presence of a maleated polypropylene in the galleries of organically-coated clay, the surfactant flattens over the silicate surface to shield the clay from the polymer despite its functional moiety. In such a case, paramagnetic interference by the silicate towards the carbon groups of the surfactant in close proximity would severely broaden and weaken any related peaks.

General discussion

It has been well established in the literature that achieving an intercalated silicate structure does not readily predispose the clay mineral to exfoliation,[28,29] but rather intercalation is a necessary mechanism towards overcoming the barriers of exfoliation. XRD results in this work have indicated that the modified clay, in the presence of a maleic anhydride grafted polypropylene compatibilizer, exhibited varying degrees of basal expansion; however, only those composite materials exhibiting major microstructural changes to the confined surfactant were notably exfoliated. With favorable interfacial interaction for all the compatibilizer species selected for this study, the constraint in their capacity to intercalate into the galleries of the clay can largely be related to their molecular size. This was most evident by the extensive intercalation and partial exfoliation of the organoclay by the oligomeric MA-PP, Li6252. For all conditions examined, this compatibilizer readily entered the galleries of the clay without aid from the supercritical solvent. However, if the intended use of a nanocomposite requires enhanced mechanical properties, then the lower molecular weight compatibilizer species would appear undesirable.

In comparison, the larger molecular size of PB3200 and PB3002 largely restricted their entry to only the outer edges of the silicate stack without $scCO_2$ aid, yielding only minor basal expansion. Most likely, the majority of associations with the clay in such cases would be confined to the broken plane of the clay which possesses suitable sites for hydrogen bonding with the compatibilizer. In the absence of $scCO_2$, the NMR and FTIR analyses suggests that these higher molecular weight compatibilizers have little or no effect on the surfactant arrangement within the clay galleries. The *in-situ* XRD analysis revealed that under these conditions without $scCO_2$ greater uniformity in the ordered structure of the silicate sheets resulted along with a small increase in basal spacing. The annealing conditions would seem to have afforded more reorganization of the surfactant in the galleries and possibly some chains of the compatibilizer entered, probably from the lower molecular weight fractions of these compatibilizers. The

poor extent of exfoliation for these higher molecular weight species was comparable to the reported results by other researchers.[9,10,12]

Larger molecules could be afforded entry to the clay galleries when annealed in the presence of the supercritical CO_2, which demonstrates the capacity of this unique solvent to act as an exfoliating agent in the synthesis of a nanocomposite. For moderate molecular sizes such as PB3200, the plasticizing features of the supercritical fluid allowed a similar extent of exfoliation as witnessed with the oligomeric species, Li6252. ^{13}C-NMR and FTIR results appear to indicate that the chains of PB3200 could become fully intercalated into the galleries of the clay, so much so that the surfactant arrangement was dramatically altered. The *in-situ* XRD characterization of the phenomenon showed substantial heterogeneity in the clay structure arising from this processing condition, though the lack of shift in the diffraction peak position suggests intercalation was localized to only a few galleries. Once a chain pushes aside the surfactant to fully intercalate and expand a gallery there is a greater tendency for subsequent intercalating chains to enter at the same location rather than randomly approaching any gallery in the stack. The length of chains for PB3002 appeared to have exceeded the upper bounds in capacity of the $scCO_2$ to aid in penetrating the galleries of C20A.

The unexpected finding in this work was that the usefulness of $scCO_2$ appeared to be constrained to the manner by which the clay was exposed to the solvent. Pretreatment of the clay with $scCO_2$ (i.e., s-C20A) offered no benefit towards greater diffusion of the compatibilizer into the clay galleries compared to an as-supplied organoclay. The basal spacing gained by pretreatment was not sufficient to afford easier access of the macromolecules into the confined spaces within the clay. Rather, annealing the two components, clay and compatibilizer, together in the presence of the $scCO_2$ was far more beneficial towards exfoliation. However, a cautionary point should be made that as these trials did not include shear, it was not possible to exclude the possibility that $scCO_2$ pretreated clays may still be more easily delaminated. This concern will be addressed in future work.

CONCLUSIONS

All three compatibilizers in this study contained sufficient polarity to interact with the silicate structure of C20A, but their abilities to intercalate varied significantly. The short chain oligomeric MA-PP, Li6252, readily entered the galleries of the clay, leading to extensive intercalation and exfoliation for all conditions examined, including those without the supercritical solvent. The larger molecular sizes of PB3200 and PB3002 had their entry into the interlayer regions restricted without $scCO_2$ assistance, yielding only minor basal expansion. The moderate molecular weight PB3200 mixture showed the strongest evidence for $scCO_2$ providing aid toward compatibilizer intercalation and achieved a similar extent of exfoliation as observed with the oligomeric species. The length of chains for PB3002 appeared to have exceeded the upper bounds in molecule size for the $scCO_2$ to aid in penetrating the galleries of C20A. Pretreating the C20A with $scCO_2$ in place of its use with both clay and compatibilizer present did not improve intercalation. The benefit of $scCO_2$ for intercalation and exfoliation was proposed to be due to its plasticizing effect on the alkyl chains of the clay surfactant and the polymer chains.

We wish to especially thank Dr. Douglas Hunter from Southern Clay Products for his assistance in the preparation of the organoclays as well for his technical advice, and Dr. Robert Berno at the McMaster NMR facilities for his advice and assistance in the solid-state NMR analysis.

References

1. Manke, C. W.; Gulari, E.; Mielewski, D. F.; Lee, E. C. U.S. Pat. No. 6,468,073, 2002 (Ford Global Technologies, Wayne State University).
2. Zerda, A. S.; Caskey, T. C.; Lesser, A. J Macromolecules 2003, 36, 1603.
3. Mielewski, D. F.; Lee, E. C.; Manke, C. W.; Gulari, E. U. S. Pat. No. 6,753,360, 2004 (Ford Global Technologies, LLC, Wayne State University).
4. Sato, Y.; Fujiwara, K.; Takikawa, T.; Sumarno, S.; Takishima, S.; Masuoka, H. Fluid Phase Equil 1999, 162, 261.
5. Nalawade, S. P.; Picchioni, F.; Janssen, L. P. B. M. Chem Eng Sci 2007, 62, 1712.
6. Kim, D. H.; Fasulo, P. D.; Rodgers, W. R.; Paul, D. R. Polymer 2007, 48, 5960.
7. Wang, Y.; Chen, F.-B.; Wu, K.-C.; Wang, J.-C. Polym Eng Sci 2006, 46, 289.
8. Hong, C. H.; Lee, Y. B.; Bae, J. W.; Jho, J. Y.; Nam, B. U.; Hwang, T. W. J Ind Eng Chem 2005, 11, 293.
9. Kato, M.; Usuki, A.; Okada, A. J Appl Polym Sci 1997, 66, 1781.
10. Kawasumi, M.; Hasegawa, N.; Kato, M.; Usuki, A.; Okada, A. Macromolecules 1997, 30, 6333.
11. Vaia, R. A.; Giannelis, E. P. Macromolecules 1997, 30, 7990.
12. Wang, Y.; Chen, F.-B.; Li, Y.-C.; Wu, K.-C. Composites: Part B 2004, 35, 111.
13. Shi, D.; Yang, J.; Yao, Z.; Wang, Y.; Huang, H.; Jing, W.; Yin, J.; Gosta, G. Polymer 2001, 42, 5549.
14. Glebov, E. M.; Krishtopa, L. G.; Stepanov, V.; Krasnoperov, L. N. J Phys Chem A 2001, 105, 9427.
15. Clark, K.; Lee, S. Polym Eng Sci 2004, 44, 1636.
16. Liu, T.; Hu, G.-H.; Tong, G.-S.; Zhao, L.; Cao, G.-P.; Yuan, W.-K. Ind Eng Chem Res 2005, 44, 4292.
17. Thompson, M. R.; Liu, J.; Krump, H.; Kostanski, L. K.; Fasulo, P. D.; Rodgers, W. R. J Colloid Interf Sci 2008, 324, 177.
18. Rogers, K.; Takacs, E.; Thompson, M. R. Polym Test 2005, 24, 423.

19. Gokel, G. W. Dean's Handbook of Organic Chemistry; McGraw-Hill: New York, 2004.
20. Thompson, M. R.; Balogh, M. P.; Speers, R.; Fasulo, P. D.; Rodgers, W. R. J Chem Phys 2009, 130, 044705.
21. Horsch, S.; Serhatkulu, G.; Gulari, E.; Kannan, R. M. Polymer 2006, 47, 7485.
22. Vaia, R. A.; Teukolsky, R. K.; Giannelis, E. P. Chem Mater 1994, 6, 1017.
23. Wang, L.-Q.; Liu, J.; Exarhos, G. J.; Flangan, K. Y.; Bordia, R. J. Phys Chem B 2000, 104, 2810.
24. De Rosa, C.; Auriemma, F.; Capitani, D.; Caporaso, L.; Talarico, G. Polymer 2000, 41, 2141.
25. Russell, K. E.; Mcfaddin, D. C.; Hunter, B. K.; Heyding, R. D. J Polym Sci B 1996, 34, 2447.
26. Walter, P.; Mäder, D.; Reichert, P.; Mülhaupt, R. J Macromol Sci A 1999, 36, 1613.
27. Toth, R.; Coslanich, A.; Ferrone, M.; Fermeglia, M.; Pricl, S.; Miertus, S.; Chiellini, E. Polymer 2004, 45, 8075.
28. Bharadwaj, R. K.; Vaia, R. A.; Farmer. B. L. In ACS Symposium Series 804: Polymer Nanocomposites; Krishnamoorti, R.; Vaia, R. A., Eds.; American Chemistry Society: Washington DC, 2002; Chapter 16, p 209–223.
29. Sinsawat, A.; Anderson, K. L.; Vaia, R. A.; Farmer, B. L. J Polym Sci Part B: Polym Phys 2004, 41, 3272.